Mikrochim. Acta 114/115, 431–440 (1994)

Mikrochimica Acta

© Springer-Verlag 1994
Printed in Austria

Structural Characterization Techniques for the Analysis of Semiconductor Strained Heterostructures

Filippo Romanato[1,**], Marina Berti[1,*], Massimo Mazzer[1], Antonio Vittorio Drigo[1], Laura Lazzarini[2], Paolo Franzosi[2], Giancarlo Salviati[2], and Daniele Bertone[3]

[1] Department of Physics, University of Padova, Via Marzolo 8, I-35131 Padova, Italy
[2] CNR-MASPEC Institute, Via Chiavari 18/A, I-43100 Parma, Italy
[3] CSELT, Via G. Reiss Romoli 274, I-10148 Torino, Italy

Abstract. A combined method for structural characterization of strained epitaxial heterostructures involving different techniques such as Rutherford backscattering spectrometry (RBS), multiple crystal X-ray diffractometry (MCD) and transmission electron microscopy (TEM) is presented. In order to obtain a complete characterization of the analysed structure, three different quantities are measured independently: the epilayer thickness, the density of misfit dislocations which may appear at the interface, and the significant components of the strain tensor, mainly the tetragonal distortion, affecting the epilayer lattice. In this way the thermodynamic state and the mechanisms of plastic deformation of the structures can be fully investigated. In this contribution we present and discuss the experimental results concerning a set of InP/GaAs samples having different layer thicknesses ranging from 5 to 500 nm. The thickness of the samples has been determined by RBS. Measurements of in-plane strain and tetragonal distortion have been performed by MCD and RBS-channelling respectively, finally TEM has been used for determining the defects densities and distribution.

Key words: structural characterization, heterostructures, InP/GaAs.

Due to the additional degree of freedom for band engineering, semiconductor based strained-layer structures are very interesting and widely studied [1]. If commensurate structures are grown, the lattice mismatch is accommodated by biaxial strain in the epilayer plane. This influences both the optical properties and the generation

* Present address: Dipartimento di Elettronica per l'Automazione, Via Branze 38, 25123 Brescia, Italy
** To whom correspondence should be addressed

of defects which may affect the device performance. For these reasons, a quantitative understanding and structural characterization of strained-layer based heterostructures is important. In particular, InP/GaAs heterojunctions have potential advantages for the integration of InP-based LASER and detectors operating at infrared wavelengths with fast GaAs field effect devices [2]. From the structural point of view, it is particularly interesting to grow binary InP films on GaAs substrates since a quite complicated mechanism of mismatch accommodation, due to the high misfit, is involved. The critical thickness for pseudomorphic growth is reached at few monolayers when the coherency between film and substrate is broken by the generation of extended defects or by the onset of 3D growth.

In this paper, the use of RBS, MCD and TEM techniques for studying InP/GaAs single layer heterostructures is presented. As a result we show that the synergy granted by the use of several complementary techniques is extremely important in this kind of analysis where the relationship between thermodynamics and kinetics is still far from being well understood.

Experimental

Growth procedures. The growth system is a home-made conventional low pressure-metal organic chemical vapour deposition (LP-MOCVD) apparatus with a fast switch gas manifold the details of which have been described previously [3]. The present atomic layer epitaxy (ALE) growth was performed by alternately introducing phosphine (PH_3) and trimethylindium (TMIn) spaced by an argon purge step. The use of Ar as carrier gas allows the monolayer saturation (i.e. ALE growth mode) to occur over a wide range of temperatures (320–360 °C). The growth temperature and the working pressure were 340 °C and 76 torr respectively. The total flow rate was 7 slpm giving a gas velocity of about 100 cm/s. Under these conditions InP layers with thickness ranging between 5 and 150 nm have been grown entirely by ALE on good quality (001) oriented GaAs substrates without depositing any buffer layer. Mixed ALE and conventional MOCVD and entirely MOCVD samples have been grown with thickness up to 500 nm.

Structural characterization. Rutherford backscattering spectra have been obtained by using a 2.00 MeV $^4He^+$ beam at the Laboratori Nazionali di Legnaro (Padova). The scattering angle was chosen at 120° in order to improve the thickness resolution for thin films. The RBS measurements were calibrated in solid angle against Ta/Si standard samples whose absolute Ta content is known with an accuracy better than 2% [4]. The beam charge collection was performed by using the whole scattering chamber as a Faraday cup, reaching an accuracy better than 1%. A high precision goniometric sample holder was used to perform the channelling analysis [5]. Three rotation axes allow complete freedom for orientation of the sample with respect to the beam. Two linear translations allow the beam spot position to be changed on the sample surface in order to avoid radiation damage accumulation during the measurements while keeping the analysed point at the intersection of the rotation axes. All the movements are operated by independent and fully computer controlled stepping motors. One step corresponds to 0.01° for each rotation axis and the repeatability and overall precision are both 0.01°.

The X-ray diffraction investigations have been performed in a high resolution diffractometer equipped with a four 220 reflections Ge monochromator. Cu $K\alpha_1$ radiation and the 004 symmetric reflection have been used to measure the component of the lattice mismatch between the epilayer and the substrate perpendicular to the interface. In order to reduce the diffuse intensity background, narrow slits were placed in front of the sample and just before the detector. In this way, very weak Bragg peaks from very thin layers can be revealed.

The transmission electron microscopy has been performed in an analytical 2000FX JEOL transmission electron microscope (TEM) with a Scherzer resolution of 3.1 Å. Conventional (CTEM) and high resolution (HREM) investigations have been carried out on (001) plan view and (110) cross section

Table 1. Structural characterization results for the samples analysed by the RBS-channelling technique

Sample no.	Growth	Thickness (nm)	ε_T (10^{-4})	$\varepsilon_\parallel$ (10^{-4})
82	ALE	20 ± 3	—	—
58	ALE	38 ± 3	93 ± 9	$-(44 \pm 4)$
183	MOCVD	301 ± 6	23 ± 3	$-(11 \pm 2)$
180	ALE + MOCVD	217 ± 3	20 ± 3	$-(9 \pm 2)$
176	MOCVD	520 ± 5	21 ± 3	$-(10 \pm 2)$

From left to right: sample identification, growth technique, film thickness, tetragonal distortion and in-plane strain. The limited RBS depth resolution does not allow to measure the tetragonal distortion of sample no. 82 without including the contribution of the heavily damaged interface layer.

oriented samples respectively. The specimens have been prepared by standard mechanochemical procedures followed by Ar^+ and I^+ ion milling [6] in a 600 DUOMILL Gatan system.

Results and Discussion

The thickness of the InP layers was mainly determined by RBS; in some cases the results have been checked by means of cross section TEM observations. In our data reduction the experimental spectrum is simulated by a computer code through the use of trial concentration profiles until agreement with the experimental spectrum, within the statistics, is obtained [7]. The results are summarised in Table 1.

A guess of the layer thickness to be used in the trial concentration profiles can be obtained from the experimental spectra either from the energy width, ΔE, of the In signal or, in the case of thin epitaxial layers, by measuring the integral under the In signal and assuming a stoichiometric composition. For a 2 MeV $^4He^+$ beam and for a scattering angle of 120° the depth resolution for InP is about 17 nm. For layers below the depth resolution, the only way for measuring the sample thickness by RBS is to calculate the integral of the In signal. Figure 1 reports the experimental spectra together with the corresponding simulations for two different samples: ALE grown Sample #82 whose thickness is about 20 nm is compared to MOCVD grown Sample #183 whose thickness is about 300 nm. In both cases the best simulation has been obtained by assuming a quite sharp interface. This means that the layer structure must be quite continuous and 3D islands are not present.

In the case of ALE grown samples, this result has been confirmed by TEM investigations of the early stages of growth revealing that even the thinnest sample is a continuous 5 nm thick layer as can be seen in Fig. 2.

This is not the case for thin MOCVD samples as shown in Fig. 3. Three features indicate that the layer is not continuous and it must consist of InP islands over the GaAs substrate. First, the InP signal is considerably lower than expected; secondly, despite the GaAs substrate should be covered by the InP layer, a tail of the As signal

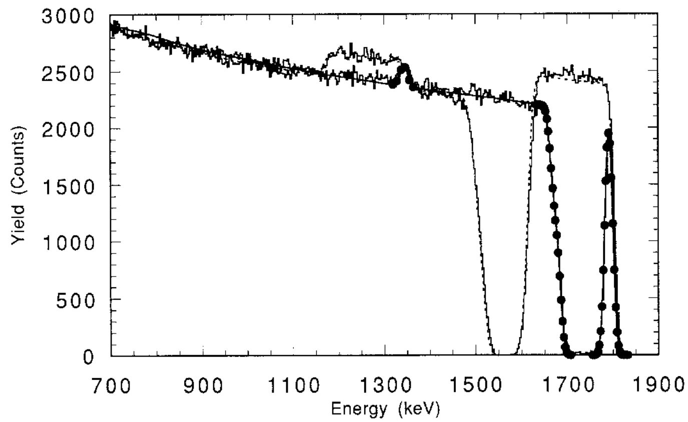

Fig. 1. Random RBS spectra together with the corresponding simulations. Dotted line: simulation of sample no. 183-MOCVD (E_0 = 2.00 MeV, θ = 170°). Circles: simulation of sample no. 82-ALE (E_0 = 2.00 MeV, θ = 120°). In both samples the interface between the InP film and the GaAs substrate is sharp

Fig. 2. (110) Bright field(BF)-zone axis HREM micrograph of an InP/GaAs 5 nm thick epilayer. The layer is continuous and no island formation is revealed

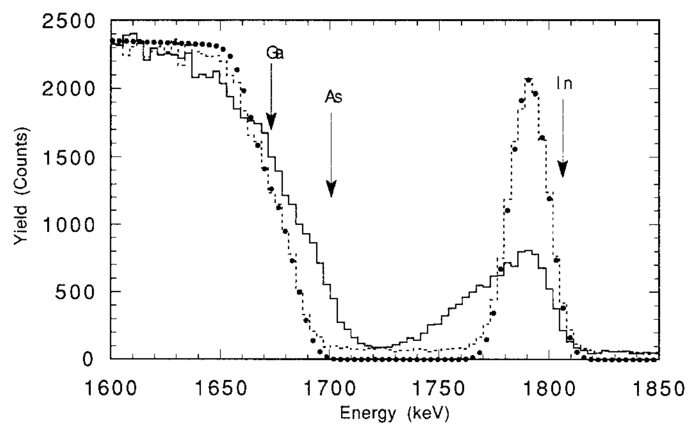

Fig. 3. Random RBS spectra (E_0 = 2.00 MeV, θ = 120°): full line: MOCVD grown InP/GaAs layer with nominal 70 nm thickness; broken line: 20 nm thick ALE grown sample; dots: the computer simulation of the ALE grown sample spectrum

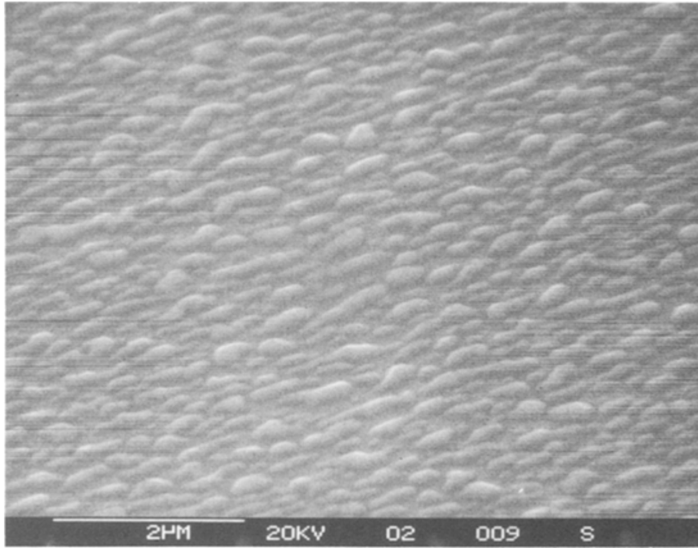

Fig. 4. Secondary electron microscopy image showing the island formation of the MOCVD growth

reaches the energy edge corresponding to the As surface scattering edge. This is a clear indication that part of the sample surface is not covered by InP. Finally, it can be argued that the islands are not uniform in thickness because of the low energy tail of the In signal. These results are supported by scanning electron microscopy (SEM) investigations. Figure 4 shows a secondary electron micrograph of the sample surface, where island formation is evident: the islands are randomly distributed in size, thickness and shape. In order to be sure that the features of Fig. 4 were actual InP islands, X-ray fluorescence investigations have been performed inside and outside the islands. As an example, Fig. 5 reports two of the corresponding energy dispersive spectrometry spectra. Even though in this case the lateral resolution is poor, different In and P content between the islands and the uncovered regions can be detected.

The residual strain has been studied by comparing the results of MCD and RBS-channelling investigations. Figure 6 reports a typical X-ray diffraction profile concerning a structure with a layer thickness of 295 nm. The origin of the horizontal axis is conventionally set at the Bragg angle θ of the GaAs substrate. The lattice parameter perpendicular to the interface $a_{\perp}$ has been measured by using a symmetric reflection. Then, the in-plane lattice parameter $a_{\parallel}$ have been calculated in the framework of the continuum elasticity theory. The results are shown in Fig. 7, where $a_{\perp}$ and $a_{\parallel}$ are reported as a function of the layer thickness t_L. Caution must be taken for the data of the lowest thickness layer because of the low intensity and the large width of the experimental peaks. It can be seen that a lattice relaxation of about 70% occur for $t_L = 23$ nm and for $t_L > 300$ nm the unit cell of the InP layer is almost completely relaxed.

Concerning the RBS-channelling analysis, the method used to determine the lattice distortion is based on a high precision measurement of the absolute angular position of a set of axial and planar channelling minima [5]. The tetragonal distortion is obtained by a least squares fitting of all the measured channelling

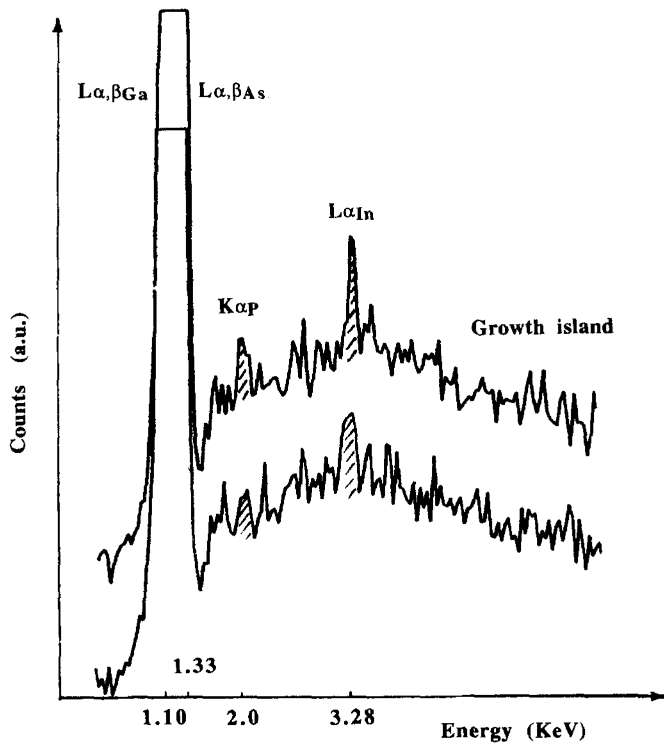

Fig. 5. The islands at the surface of the samples are composed by InP as it is demonstrated by the ED spectra taken inside and outside the islands

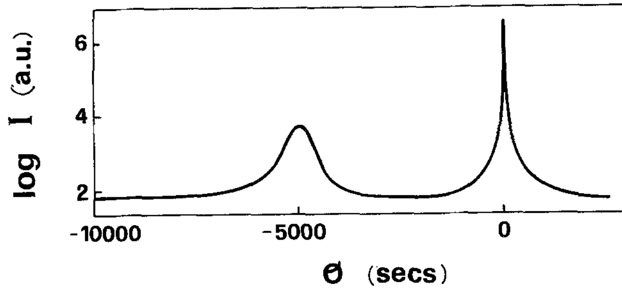

Fig. 6. Typical X-ray experimental diffraction profile of a 295 nm InP/GaAs thick layer.

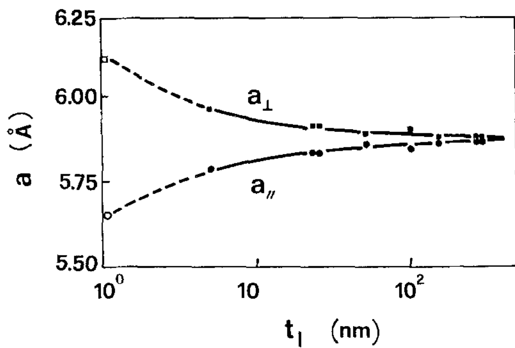

Fig. 7. Lattice parameter of the epilayer perpendicular and parallel as a function of the layer thickness

minima. If θ is the angle of a given lattice direction with respect to the surface normal and $\Delta\theta$ is the measured angular deviation due to the deformation, the tetragonal distortion is given by:

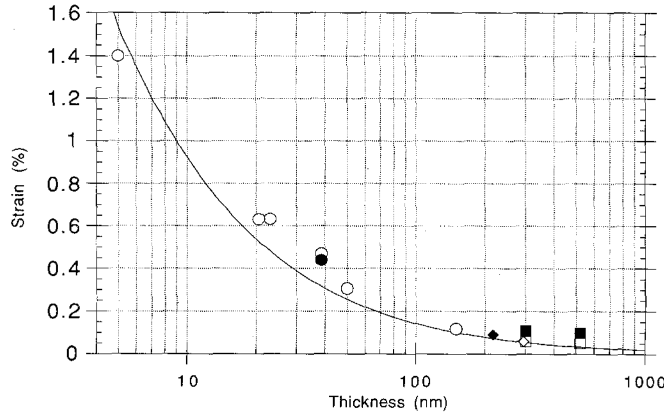

Fig. 8. Measured residual strain as a function of the layer thickness of the whole set of investigated samples. Different growth are indicated by: O ALE, □ MOCVD, ◇ ALE + MOCVD. A further distinction is between open symbols and full symbols that correspond to X-ray diffraction multiple crystal and RBS channelling measurements respectively; solid line: Matthews and Blakeslee equilibrium theory prediction

$$\varepsilon_T = \frac{a_\perp - a_\parallel}{a_\parallel} = -\frac{2\,\Delta\theta}{\sin 2\theta}. \tag{1}$$

For a (001) grown structure, the in-plane strain $\varepsilon_\parallel$, is related to the tetragonal distortion through the equation:

$$\varepsilon_\parallel = -\frac{\varepsilon_T}{1 + 2\dfrac{c_{12}}{c_{11}}}, \tag{2}$$

where c_{12} and c_{11} are the elastic (stiffness) constants.

The results of this study are summarised in Table 1 and they are reported in Fig. 8 together with the MCD results and the theoretical predictions of the equilibrium theory of Matthews and Blakeslee [8]. In order to be compared to the theoretical curve, the experimental points should be corrected for the residual thermal strain which is of the order of some 10^{-4} [9] and depends on the growth temperature. However, apart from this minor correction, we can conclude that the residual strain as a function of the layer thickness follows quite well the predicted trend. Moreover, no significant differences among samples grown by different techniques (ALE, MOCVD or ALE + MOCVD) is observed .

A check of the crystalline quality of the samples has been performed by analysing the [001] axial channelling spectra both of the epilayers and of a bulk InP substrate. The normalised yield ratio between the aligned and random spectra (χ) provides information on the crystal defect profiles.

Figure 9 reports the χ values as a function of the layer thickness for a 300 nm and a 520 nm thick MOCVD grown InP epitaxial layers, together with the χ values for a InP substrate as a reference. It is evident from the figure that the surface quality of the two films is comparable to the bulk InP, the normalised yields of the layers being only slightly higher than that of the bulk crystal. On the contrary, in a region

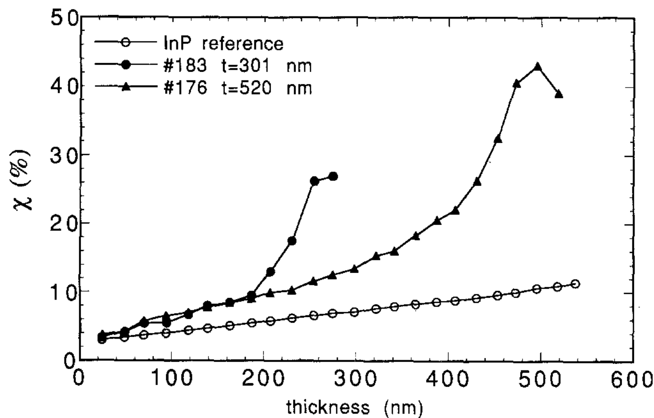

Fig. 9. χ is the dechannelling yield from In signal for MOCVD grown samples as a function of depth. Open dots: reference InP sample; full dots: sample no. 183, 301 nm thick; full triangles: sample no. 176, 520 nm thick

near to the interface, approximately 50 nm thick, the yield increases abruptly, indicating the presence of a noticeable concentration of defects, in particular misfit dislocations (MD), whose nucleation is expected when the layer thickness exceeds a few monolayers due to the large lattice mismatch between InP and GaAs.

In this respect, the cross sectional TEM observations confirm these results, indicating that the distribution of the crystal defects across the epilayer is not uniform [10]. A very large density of MD is observed at the interface. Moreover, planar defects (PD) such as stacking faults and microtwins, originating at the interface and propagating along the $\{111\}$ planes, affect all the investigated layers. Finally, threading dislocations (TD) have been revealed in specimens thicker than 70 nm. The PD and TD density decreases from the interface region to the top of the layers due to annihilation reactions. HRTEM investigations showed an average linear MD density varying from about $8\text{–}9 \times 10^5$ cm^{-1} in the thinnest sample to 2×10^6 cm^{-1} in the almost completely relaxed thickest layers. These results agree fairly well with the estimation obtained from the in-plane strain measurements by assuming that strain is released only by 60° type MD. The nature of the MD was determined by constructing Burgers circuits on HREM micrographs. In all the investigated specimens the great majority of MD are of the 60° type even if some 90° type MD were also observed in the thickest layers [11].

On the basis of the above results we can conclude that, as far as strain relaxation is concerned, the behaviour of the investigated samples is independent of the growth conditions (i.e. ALE, ALE + MOCVD, MOCVD). On the other hand, TEM investigations have revealed a reduction of the PD density in the mixed ALE + MOCVD samples (Fig. 10 a) with respect to the totally ALE grown layers (Fig. 10 b), most likely as a consequence of the higher growth temperature. This fact confirms the previous result [11] that planar defects seem to play no significant role in the strain release process.

Conclusions

A set of InP/GaAs samples grown by ALE and MOCVD have been analysed by different structural techniques. While ALE gives rise to layer by layer 2D epitaxy, MOCVD growth begins with island formation and layer by layer growth is restored above a 2D–3D "transition" thickness. For larger thicknesses, strain relaxation

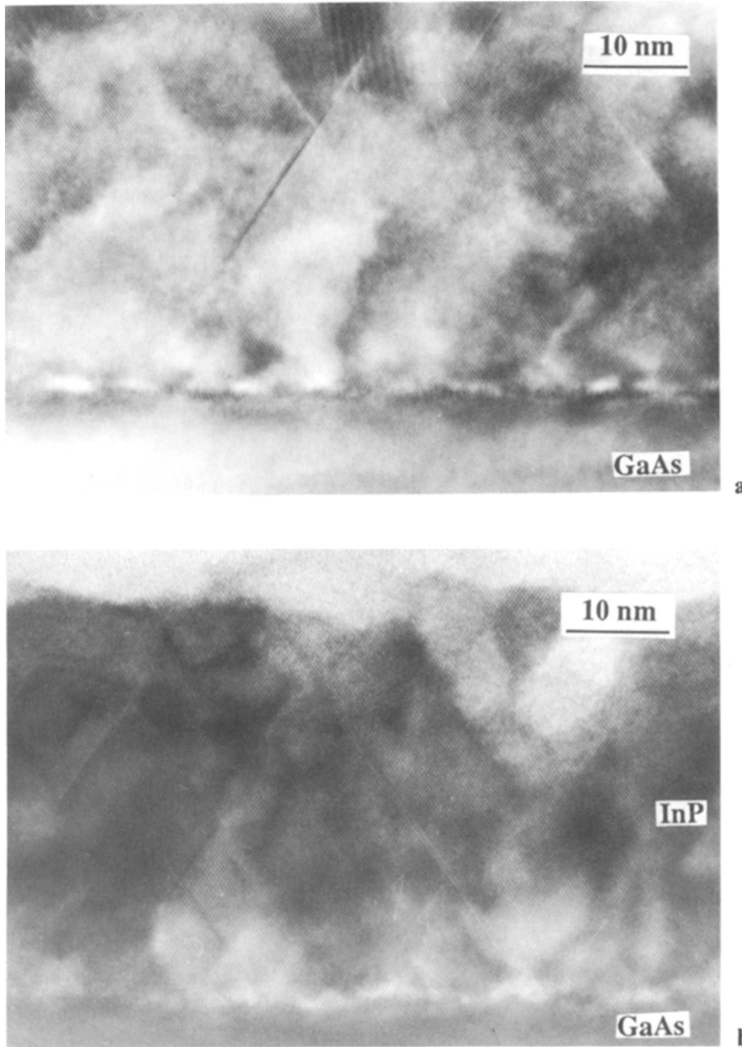

Fig. 10. Typical PD distribution in an ALE + MOCVD grown InP layer (**a**) compared with a totally ALE grown sample (**b**). The PD density reduction is apparent

seems to be independent of the growth technique and agrees quite well with the predictions of the thermodynamic equilibrium theories. It is worth noting that this behaviour is quite different with respect to other systems, grown on the same substrate, such as for instance InGaAs/GaAs [12] where strain relaxation occurs at a lower rate with increasing film thickness. Different growth kinetics together with the existence of additional degrees of freedom for mismatch accommodation in ternary layers may explain this different behaviour. Work is in progress in order to extend the analysis to other materials and mismatch regimes.

References

[1] G. C. Osbourn, *J. Vacuum Sci. Technol. B* **1983**, *1*, 379.
[2] S. J. J. Teng, J. M. Ballingal, F. J. Rosenbaum, *Appl. Phys. Lett* **1986**, *48*, 1217.

[3] D. Bertone, *J. Electronic Mat.* **1992**, *21*, 265.
[4] C. Cohen, J. A. Davis, A. V. Drigo, T. E. Jackman, *Nucl. Instrum. Meth.* **1983**, *218*, 147.
[5] A. Carnera, A. V. Drigo, *Nucl. Instrum. Meth.* **1990**, *B44*, 531.
[6] A. G. Cullis, N. G. Chew, *Mat. Res. Soc. Symp. Proc.* **1988**, *115*, 3.
[7] A. Armigliato, M. Servidori, F. Cembali, R. Fabbri, R. Rosa, A. V. Drigo, M. Mazzer, F. Romanato, S. Frabboni, R. Balboni, *Microscopy, Microstruct. Microanal.* **1992**, *3*, 363.
[8] J. W. Matthews, A. E. Blakeslee, *J. Cryst. Growth* **1974**, *27*, 118.
[9] O. Madelung (ed.), *Semiconductors*, Springer, Berlin Heidelberg New York Tokyo, 1991.
[10] M. S. Abrahams, J. Blanc, C. J. Buiocchi, *Appl. Phys. Lett.* **1972**, *21*, 185.
[11] L. Lazzarini, P. Franzosi, C. E. Norman, G. Salviati, D. Bertone, *J. Electroch. Soc.* **1993**.
[12] A. V. Drigo, A. Aydinly, A. Carnera, F. Genova, C. Rigo, C. Ferrari, P. Franzosi, G. Salviati, *J. Appl. Phys.* **1989**, *66*, 1975.